ACCOUNTS
of chemical research

Effect of Covalent Chemistry on the Electronic Structure and Properties of Carbon Nanotubes and Graphene

ELENA BEKYAROVA,[†,‡] SANTANU SARKAR,[†,‡] FEIHU WANG,[†,§] MIKHAIL E. ITKIS,[†,‡] IRINA KALININA,[†,‡] XIAOJUAN TIAN,[†,∥] AND ROBERT C. HADDON*[,†,⊥]

[†]*Center for Nanoscale Science & Engineering,* [‡]*Department of Chemistry,* [§]*Department of Physics and Astronomy, and* [∥]*Department of Chemical & Environmental Engineering, University of California, Riverside, California 92521, United States, and* [⊥]*Department of Physics, King Abdulaziz University, Jeddah 21589, Saudi Arabia*

RECEIVED ON JUNE 15, 2012

CONSPECTUS

In this Account, we discuss the chemistry of graphitic materials with particular reference to three reactions studied by our research group: (1) aryl radical addition, from diazonium precursors, (2) Diels–Alder pericyclic reactions, and (3) organometallic complexation with transition metals. We provide a unified treatment of these reactions in terms of the degenerate valence and conduction bands of graphene at the Dirac point and the relationship of their orbital coefficients to the HOMO and LUMO of benzene and to the Clar structures of graphene.

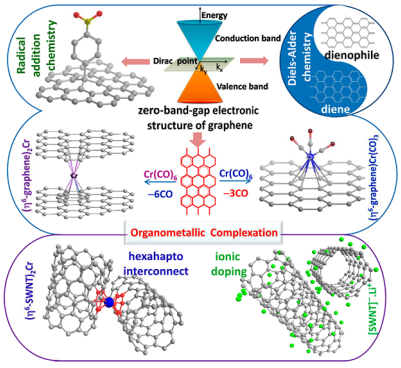

In the case of the aryl radical addition and the Diels–Alder reactions, there is full rehybridization of the derivatized carbon atoms in graphene from sp^2 to sp^3, which removes these carbon atoms from conjugation and from the electronic band structure of graphene (referred to as destructive rehybridization). The radical addition process requires an electron transfer step followed by the formation of a σ-bond and the creation of a π-radical in the graphene lattice, and thus, there is the potential for unequal degrees of functionalization in the A and B sublattices and the possibility of ferromagnetism and superparamagnetism in the reaction products.

With regard to metal functionalization, we distinguish four limiting cases: (a) weak physisorption, (b) ionic chemisorption, in which there is charge transfer to the graphitic structure and preservation of the conjugation and band structure, (c) covalent chemisorption, in which there is strong rehybridization of the graphitic band structure, and (d) covalent chemisorption with formation of an organometallic hexahapto-metal bond that largely preserves the graphitic band structure (constructive rehybridization). The constructive rehybridization that accompanies the formation of bis-hexahapto-metal bonds, such as those in (η^6-SWNT)Cr(η^6-SWNT), interconnects adjacent graphitic surfaces and significantly reduces the internanotube junction resistance in single-walled carbon nanotube (SWNT) networks. The conversion of sp^2 hybridized carbon atoms to sp^3 can introduce a band gap into graphene, influence the electronic scattering, and create dielectric regions in a graphene wafer. However, the organometallic hexahapto (η^6) functionalization of the two-dimensional (2D) graphene π-surface with transition metals provides a new way to modify graphitic structures that does not saturate the functionalized carbon atoms and, by preserving their structural integrity, maintains the delocalization in these extended periodic π-electron systems and offers the possibility of three-dimensional (3D) interconnections between adjacent graphene sheets. These structures may find applications in interconnects, 3D-electronics, organometallic catalysis, atomic spintronics and in the fabrication of new electronic materials.

1. Introduction

In 2004, it became clear that graphene and silicon share a number of features – acceptable mobilities ($\mu \geq 1000$ $cm^2/V\ s$)[1,2] were evident in the first papers, but another important characteristic was the availability of graphene wafers and this motivated the idea that it might be possible to design and build integrated circuits starting from a graphene wafer, just as the electronics industry does today

Published on the Web 11/01/2012 www.pubs.acs.org/accounts
10.1021/ar300177q

with silicon wafers.[3] Very few electronic materials are available as high purity, macroscopic 2-D crystalline wafers, and the realization of large area, high quality graphene films naturally addresses some of the objections to integrated molecular electronic devices and associated high level circuitry.[4]

Nevertheless, many problems remain in engineering the appropriate electronic components out of a graphene sheet, including the production of graphene semiconductors with a suitable energy gap and high mobility, the production of wires or interconnects of sufficient current carrying capacity, and the realization of insulating or dielectric graphene regions. Fabrication remains a particularly daunting challenge, and new lithographic processes based on organic chemistry must be developed. In this latter respect, chemical functionalization is emerging as a vital tool and it is already clear that it will assume an increasingly important role in this endeavor.[5−7] While ionic chemistry (doping, charge transfer) can serve to increase the conductivity of graphene ribbons, the role of such approaches in achieving high performance electronics remains problematic. Covalent chemistry has already been shown to modify the electronic and magnetic properties of graphene; there appears to be some hope for introducing a band gap into graphene and producing semiconductors, and the development of insulating graphene regions by the conversion of conjugated carbon atoms to sp^3 hybridization is well documented.[8−11] In almost all instances, the application of covalent chemistry, in which the sp^2 carbon atoms become rehybridized, leads to a reduction in the mobility of the charge carriers and the conductivity of graphitic materials.[12] Furthermore the use of bulk metal contacts to such materials is inevitably associated with Joule heating and is limited by the quantum conductance at the metal−carbon junction,[13] which poses difficult questions regarding the nature of the interconnects between graphitic surfaces in graphene-based electronic circuitry.

In the present Account, we discuss three graphene functionalization schemes, which have been introduced by our group: the first two of these chemistries involve the full rehybridization of the graphitic carbon atoms from sp^2 to sp^3 and result in a decrease in the conductivity and mobility of the funtionalized graphene sheet. We begin by discussing nitrophenyl functionalization of graphene,[14] which, because it proceeds by single site radical addition involving the formation of π-radicals, allows the possibility of a product containing residual spins that couple so as to allow the observation of room temperature ferromagnetism.[6,10,15]

Graphene is able to function as both diene and dienophile when paired with an appropriate Diels−Alder partner, and we have shown that this chemistry is facilitated by the electronic structure of graphene at the Dirac point.[16,17] In the present Account, we extend this concept to rationalize the chemistry of all reactions discussed herein. Finally, we close with a discussion of our recent discovery of the rich organometallic chemistry of graphitic systems, which allows the use of covalent hexahapto-metal bonds to extend the electronic structure of these π-structures into the third dimension and to interconnect the surfaces of adjacent carbon materials that contain the benzenoid ring system.[18−22] Because the degree of rehybridization at the site of complexation is insufficient to saturate the conjugated electronic structure, we refer to this latter process as constructive rehybridization, in contradistinction with the nitrophenyl addition and Diels−Alder reactions, which bring about destructive rehybridization of the graphitic structure (the derivatized carbon atoms become saturated and are effectively removed from conjugation).[21]

2. Electronic Band Structure and Chemical Reactivity of Graphene

The band structure of graphene has been extensively reviewed in the literature,[23,24] and we have recently discussed its relevance to the Diels−Alder chemistry of graphene.[17] In the present Account, we extend this analysis to show that it is possible to develop a unified treatment of the chemical reactivity of graphene based on its electronic band structure and we illustrate this approach by its application to the three chemical reactions discussed in this Account.

In Figure 1, we present the simple tight binding band structure of graphene at the level of HMO theory, which shows the dispersions of the π-bands along the high symmetry directions in *k*-space[17,23,24] together with the HMO energy levels for benzene, the allyl radical, and trimethylenemethane diradical. It may be seen that the work function of graphene ($W \approx 4.6$ eV) is defined by the crossing of the valence and conduction bands at the Dirac point (*K*), and this corresponds to the level of the nonbonding molecular orbital (NBMO = $-W$) in HMO theory and also serves to define the HOMO and LUMO of graphene. We have previously argued that the occurrence of a very high lying HOMO and low lying LUMO in graphene in conjunction with the orbital symmetries at the Dirac point is responsible for the facile reactivity of graphene in a variety of Diels−Alder reactions.[16,17]

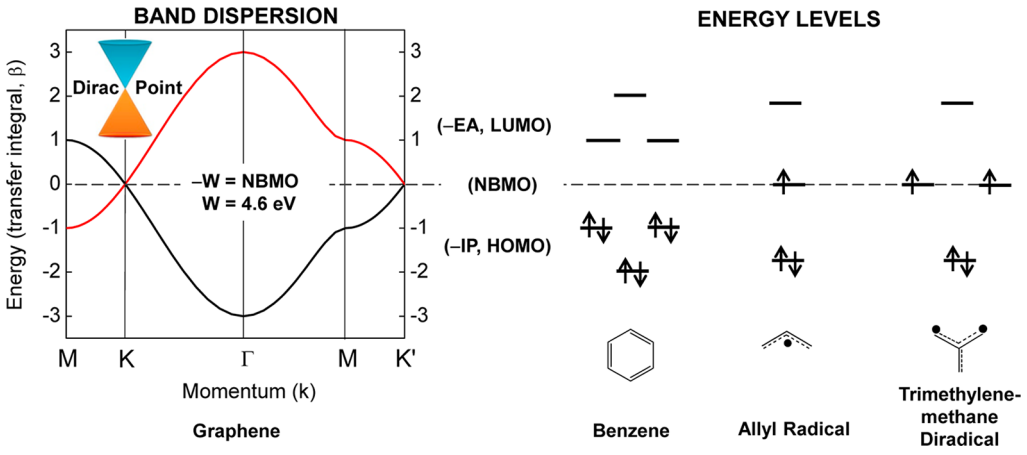

FIGURE 1. Electronic band structure of graphene, at the level of simple tight-binding (HMO) theory,[17] together with HMO energy levels for benzene, allyl radical, and trimethylenemethane diradical.

The orbitals at the Dirac point in graphene and their relationship to the HOMOs and LUMOs of benzene are given in Figure 2; these orbitals correspond to the frontier molecular orbitals (FMOs) of graphene and we have argued that they dictate the chemistry,[16,17] and we further develop this point below in conjunction with specific reactions.

3. Radical Addition Chemistry of Graphene

A number of groups have explored chemical reactions that involve the addition of radical species to graphene and this chemistry may be traced to the radical fluorination,[9] hydrogenation,[8] and hydrogen chemisorption defect[25] of graphene and graphite. The diazonium chemistry of graphitic materials is well established[26−28] and has provided a convenient route to radical addition products as a result of electron transfer to the diazonium cation (exemplified by the *p*-nitrophenyl in Scheme 1),[14] followed by loss of nitrogen to give highly reactive aryl radicals; as we have emphasized, most of the radical reactions pass through common intermediates starting with the π-radical (**2**), in which the spin is delocalized over more than 10 000 carbon atoms (Scheme 1).[6,10]

The π-radical (**2**) is an odd-alternant hydrocarbon (OAH), and just as in the case of the allyl radical shown in Figure 1 the unpaired spin resides in a nonbonding molecular orbital (NBMO),[10] and the relationship to the electronic structure of graphene is clear. This state lies at the Fermi level in graphitic samples containing the hydrogen chemisorption defect and is observable in STM images as a threefold symmetric superlattice in the local density of states (LDOS) in both tunneling directions.[25]

Assuming that the first radical addition occurs in the A-sublattice as in **2**, two distinct electronic structures may result from the second radical addition process. In the presence of small substituents, thermodynamic considerations favor

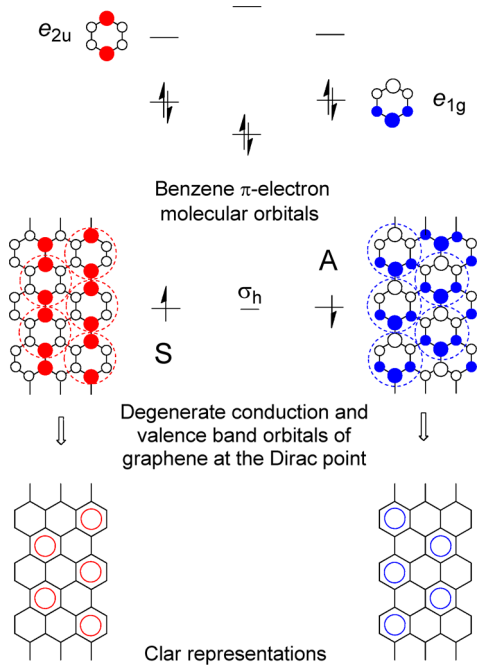

FIGURE 2. HMO energy levels of benzene and their symmetry, together with the orbital coefficients of HOMO and LUMO that map onto the degenerate conduction and valence bands of graphene at the Dirac point. These orbitals comprise the FMOs of graphene,[17] and because the e_{2u} benzene LUMO is placed in the lattice in a bonding configuration with nearest neighbors, while the e_{1g} benzene HOMO enters the lattice in an antibonding relationship with nearest neighbors, they result in a pair of degenerate orbitals at the NBMO level [Dirac point (*K*), Figure 1]. Furthermore, these FMOs map directly onto the Clar representation of graphene and clearly motivate its chemical reactivity.[16,18,19,24]

addition in the B-sublattice to give a diamagnetic product with an energy gap, as exemplified by structure **3**;[29] however, the steric bulk of the nitrophenyl group militates against the preferred 1,2- or 1,4-addition product and thus there is the possibility of structures such as **4,** which involve addition in the same

SCHEME 1. Structures of the Initial Nitrophenyl Addition Products of Graphene Following Spontaneous Electron Transfer from Graphene to the *p*-Nitrobenzene Diazonium Salt[a]

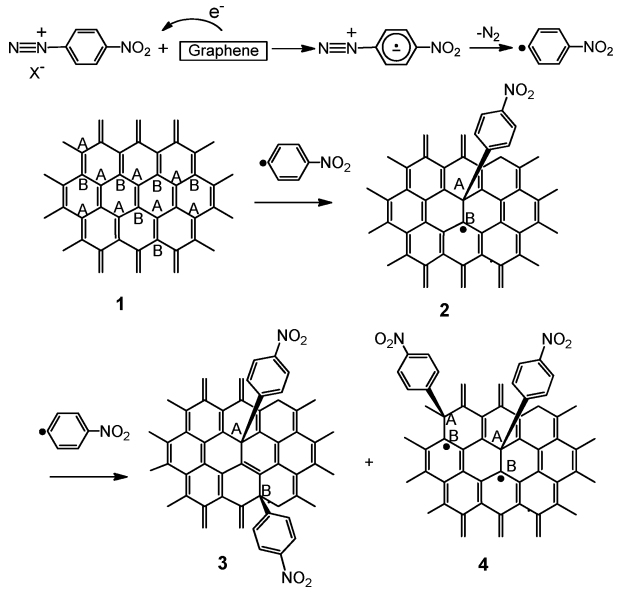

[a]The π-radical (**2**) is paramagnetic with a highly delocalized electronic structure and the spin resides in an NBMO (simplified as the allyl radical in Figure 1). The product structure represented by **3** is expected to be diamagnetic due to the antiferromagnetic coupling between the A and B graphene sublattices, while the structure represented by **4** gives rise to a diradical with a triplet ground state due to the ferromagnetic coupling between spins in the B sublattice (simplified as the trimethylenemethane diradical in Figure 1). Modified from ref 10. Copyright 2011 American Chemical Society.

sublattice. The spin count in the product increases with each radical functionalization process, which occurs in a given sublattice (without compensation by an accompanying radical addition in the other sublattice), and each spin resides in a NBMO; for biradical structures such as **4**, the simplest molecular analogue is trimethylenemethane (Figure 1).[30] Thus, at the very simplest level of tight binding HMO theory, the electronic structure of the various graphene open shell products is one in which the spins reside in NBMOs, which in the solid state lie at the Fermi level. More rigorous treatments modify this picture, but many of the qualitative conclusions remain valid; one of the more important theoretical results is the finding that the spins in these NBMOs couple ferromagnetically, because the unpaired electrons all lie in the same sublattice and this mode of coupling minimizes electron repulsion effects according to Hund's rule.[31,32]

Vibrating sample magnetometry (VSM) measurements of nitrophenyl functionalized epitaxial graphene (NP-EG) samples show that the kinetic product (**4**, attachment of the radical to a single sublattice of graphene) can be observed and such NP-EG samples show a nonlinear hysteretic dependence on magnetic field strength.[15] Figure 3 shows the nonlinear magnetization of an EG sample before (a, pristine EG)

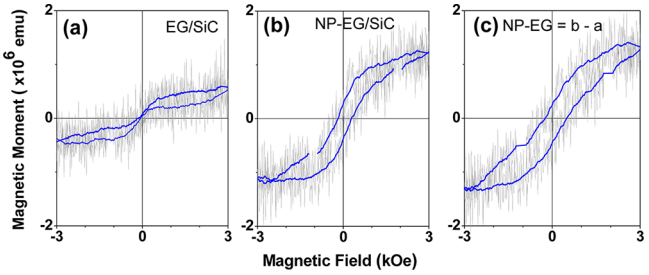

FIGURE 3. In-plane magnetization at 300 K of epitaxial graphene, EG: (a) before and (b) after nitrophenyl functionalization; (c) signal from the functionalized top graphene layer obtained by subtracting (a) from (b); the linear term due to the diamagnetism of SiC is subtracted from both (a) and (b).

and after functionalization (b, NP-EG), as a function of the magnetic field at room temperature. The difference in the magnetization data between the pristine (Figure 3a) and the nitrophenyl functionalized EG (Figure 3b) is due to the change in the magnetic properties of the graphene as a result of nitrophenyl functionalization of the top graphene layer (NP-EG, Figure 3c). The coercivity and saturation magnetization are found to be sample dependent,[15] and the factors governing the preferential sublattice functionalization remain to be understood.[6,10]

4. Diels–Alder Chemistry of Graphene

The dual nature of the Diels–Alder reactivity of graphene is apparent from a consideration of the graphene electronic structure at the Dirac point (Figure 2); because the graphene FMOs consist of a half occupied pair of degenerate orbitals, the orbital occupancies may be matched to those of the Diels–Alder partner (Figure 4),[16,17] according to the Woodward–Hoffmann rules[33] and the Frontier Molecular Orbital Theory.[34,35]

Unlike the radical addition chemistry discussed above, the Diels–Alder reactions are expected to give rise to diamagnetic 1,2- and 1,4-addition products (analogous to **3** in Scheme 1). Thus, the unique electronic structure at the Dirac point allows graphene to participate in surprisingly mild basal plane chemistry such as the Diels–Alder reaction, which we experimentally demonstrated with tetracyanoethylene and maleic anhydride (dienophiles) and 2,3-dimethoxydibutadiene and 9-methylantracene (dienes).[16] The products of the Diels–Alder reaction with graphene readily undergo a thermal retro-Diels–Alder reaction; the versatility of this covalent carbon–carbon bond formation chemistry and the dual behavior of graphene as either diene or dienophile in this chemistry (Figure 5) allows covalent grafting of a wide variety of functional groups as dienes or dienophiles and consequently provides a convenient

platform for the application of this chemistry in various postgrafting modifications of graphene for sensing and advanced materials applications.

5. Organometallic Chemistry of Graphitic Materials: Bonding, Electronic Structure, Atomic Contacts and Interconnects

The covalent bonds formed by radical addition and Diels–Alder chemistry modify the conjugated graphene sheet by the conversion of the carbon atoms at the sites of attachment from sp^2 to sp^3 hybridization and effectively remove these atoms from conjugation (referred to as destructive rehybridization).[21] This is desirable from the standpoint of band gap engineering, but in the products isolated to date the conductivity and mobility are reduced; if ordered structures can be achieved,[36] the materials performance may improve. In this final functionalization section, we introduce a further mode of covalent bonding that allows constructive rehybridization of the derivatized carbon atoms, preserves the conjugation and allows the functionalized carbon atoms to remain a part of the electronic band structure.

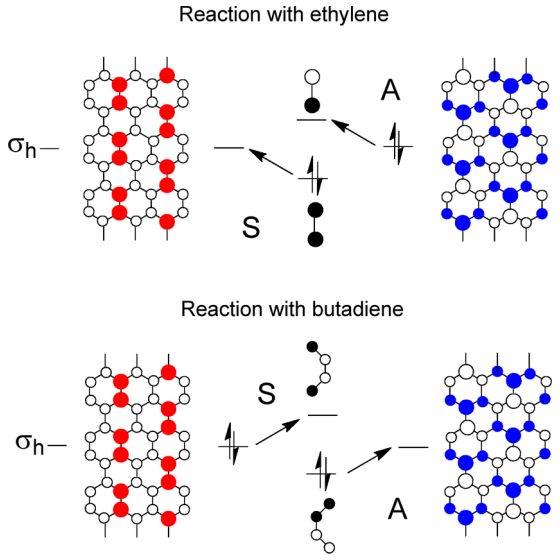

FIGURE 4. Orbital symmetry correlation diagram for the Diels–Alder reaction of ethylene and butadiene with graphene; the graphene FMOs are taken from the degenerate conduction and valence bands at the Dirac point (Figures 1 and 2).[17] Modified from ref 17. Copyright 2012 American Chemical Society.

5.1. Mono-Hexahapto-Metal Bonding. Metal atoms are usually considered to interact with graphitic surfaces in three distinct bonding configurations: (a) weak physisorption, in which there is little charge transfer or rehybridization of the graphitic carbon atoms, (b) ionic chemisorption, in which there is pronounced charge transfer to the graphitic structure with preservation of the conjugation and band structure, and (c) covalent chemisorption, in which there is significant rehybridization of the graphitic band structure and some degree of charge transfer.[37–42] Ionic chemisorption (b) can lead to the formation of salts, in which a large amount of charge is transferred to the graphitic structure and such doped materials are often associated with enhanced conductivities and even metallic and superconducting properties.[43–45] Covalent chemisorption (c) on graphitic structures can lead to a drastic modification of the bonding and a number of metals are associated with the formation of carbides. Recently, we reported a new mode of covalent chemisorption

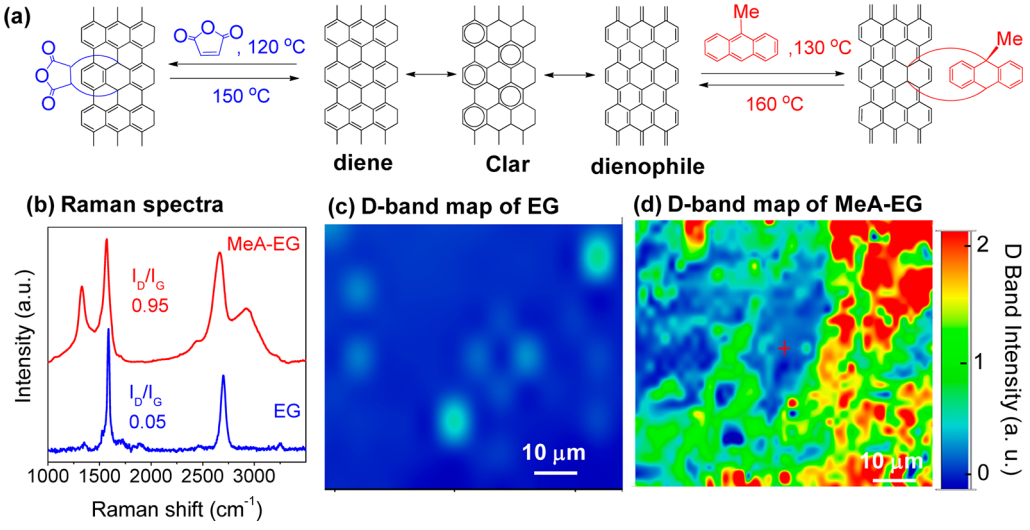

FIGURE 5. (a) Schematic of the Diels–Alder reaction of graphene with maleic anhydride (MA, dienophile) and 9-methyantracene (MeA, diene). (b) Raman spectra of epitaxial graphene (EG) in pristine form and after reaction with MeA (MeA-EG). Maps of the D-band intensity of (c) pristine EG and (d) MeA-EG. Reprinted with permission from ref 7. Copyright 2012 Elsevier.

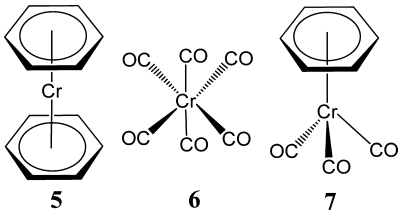

FIGURE 6. Structures of $(\eta^6\text{-}C_6H_6)_2Cr$ (**5**), $Cr(CO)_6$ (**6**), and $(\eta^6\text{-}C_6H_6)Cr(CO)_3$ (**7**).

on graphitic surfaces (d), which is based on organometallic chemistry and makes use of the hexahapto-metal bond to electronically conjugate adjacent carbon surfaces which contain the benzenoid ring system.[18−22]

In order to electronically couple the surfaces of graphitic materials, which are composed of polycyclic benzenoid ring systems, it is appropriate to begin with transition metals that are known to form bis-hexahapto-metal bonds, as exemplified by bis(benzene)chromium $[(\eta^6\text{-}C_6H_6)_2Cr]$ (**5**, Figure 6), and there are many metals known to form such bonds, which are therefore candidates for this application.[46]

Based on the gas phase structure of this compound,[47] the pyramidalization angle[48] is calculated to be $\theta_P = 1.7°$, in the sense that the hydrogen atoms tilt toward the metal atom, compared to the normal tetrahedral angle of $\theta_P = 19.5°$ for sp^3 hybridized carbon. In the highly condensed systems considered here, in which the network of benzene rings is quite rigid, the degree of pyramidalization estimated above represents an upper bound and there will be very little geometric distortion on metal complexation of the graphitic benzenoid ring systems. Nevertheless, these bonds are strong,[49] allow the metal d-orbitals to couple to the π-systems while preserving the band structure, and, as we show below, are effective in electrically interconnecting graphitic surfaces.[18−22]

We have used solution, solid state and gas phase chemistries to prepare a series of organometallic derivatives of samples of graphene, graphite, and single-walled carbon nanotubes (SWNTs), which in all cases show a measurable effect on the electrical conductivity as a result of the ability of the hexahapto-metal bond to attach to and, in some cases, interconnect the surfaces of extended, periodic π-electron systems.[18−22]

Our work on the organometallic chemistry of graphitic materials began with the solution chemistry of graphene, graphite, and SWNTs, and we found that all of these forms of conjugated carbon materials underwent reaction when treated with chromium hexacarbonyl [$Cr(CO)_6$, **6**] and benzene chromium tricarbonyl [$(\eta^6$-benzene)$Cr(CO)_3$, **7**] (Scheme 2), and the degree of reaction was determined by the surface

SCHEME 2. Reactions of Graphene and SWNTs[a]

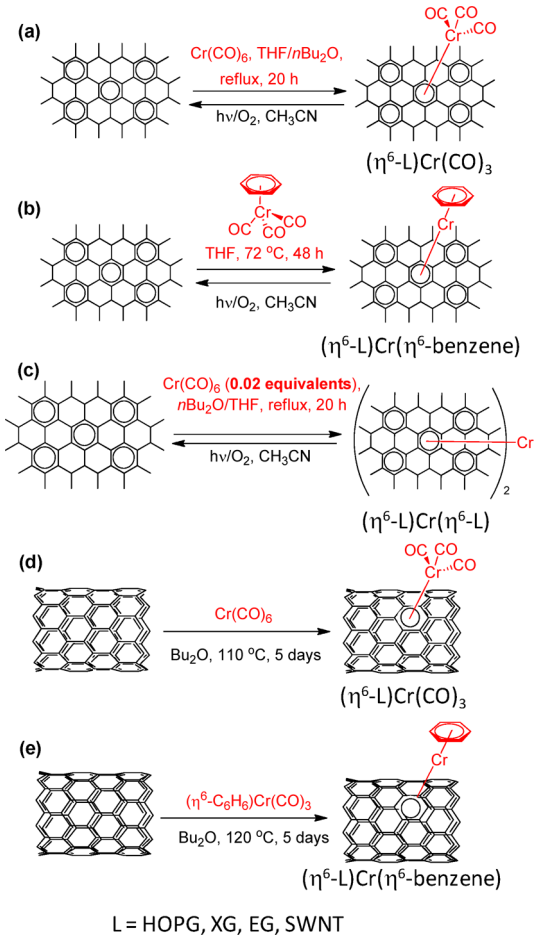

[a]Reactions of graphene with (a) chromium hexacarbonyl, (b) $(\eta^6$-benzene)$Cr(CO)_3$, and (c) with chromium hexacarbonyl in the presence of excess exfoliated graphene (XG) to give the fully graphene-coordinated material, $(\eta^6\text{-XG})Cr(\eta^6\text{-XG})$. Reactions of SWNTs with (d) chromium hexacarbonyl and (e) $(\eta^6$-benzene)$Cr(CO)_3$.

presentation of the carbon materials and their solubility in the reaction medium.[18,19]

The use of soluble carbon nanotubes [SWNT-CONH-$(CH_2)_{17}CH_3$][50] allowed the isolation of materials with a significant chromium content, and because the products of these reactions remained soluble in organic solvents, we were able to carry out a detailed characterization of these new materials.[18,19] Based on the chromium content in the compounds, their response to decomplexation reactions with mesitylene, transmission electron microscopy, and our analysis of the bonding, we concluded that both exohedral and endohedral modes of complexation were operative in these reactions (Scheme 3),[19] together with metal cluster formation.

We have argued[18−22] that the use of the organometallic hexahapto-metal bond is a particularly useful approach to the functionalization of graphitic carbon materials because

the conjugation and band structure of the carbon substrate are left relatively unperturbed,[37,40] in contrast with the σ-bond forming reactions discussed above, which lead to destructive rehybridization of the carbon atoms of the graphitic surface. In previous studies of SWNT reactions, we were able to clearly distinguish the effects of ionic and covalent functionalization processes by using UV−vis-NIR-FIR spectroscopy to follow the response of the SWNT interband electronic transitions to chemistry.[51] Ionic chemistry (doping) is characterized by a progressive reduction of the oscillator strength of the interband electronic transitions of the semiconducting SWNTs (first S_{11}, and then in some cases S_{22}; Figure 7a), and for oxidative charge transfer from the SWNTs this is due to the depletion of the first valence band in the SWNTs (S_{11}, Figure 7b, doped semiconducting SWNTs); the spectral weight of these transitions is transferred to the far IR, due to additional transitions at the Fermi level (M_0, Figure 7c, and S_{1fc}, Figure 7b). Whereas the formation of σ-bonds to the SWNT side-walls drastically reduces the strength of the metallic transitions (M_0) by introduction of a band gap and also weakens the semiconducting transitions (S_{11} and S_{22}) as the sites of functionalization act as defects, which destroy the translational invariance of the lattice. As may be seen in the spectra shown in Figure 8, the interband transitions of the functionalized SWNTs are uniformly weakened but not removed by the hexhapto-Cr-bond forming reactions.

SCHEME 3. Hybrid Orbitals of the SWNT Carbon Atoms Involved in Overlap with the Metal d-Orbitals in η^6-SWNT Complexes[a]

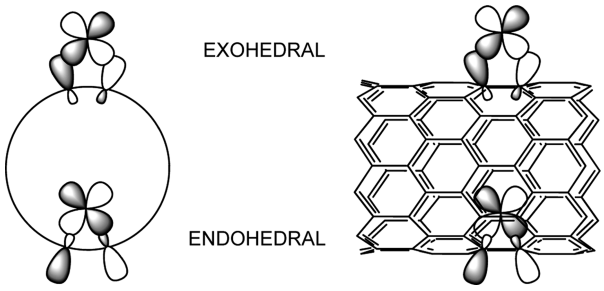

[a]Reprinted from ref 19. Copyright 2012 Wiley.

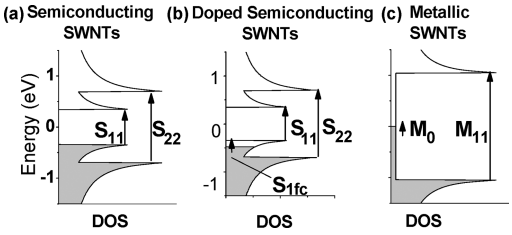

FIGURE 7. Density of states (DOS) as a function of energy for (a) semiconducting, (b) doped semiconducting, and (c) metallic SWNTs, together with interband transition (S_{11}, S_{22}, and M_{11}; near IR) and free carrier (S_{1fc} and M_0; far IR) excitations.

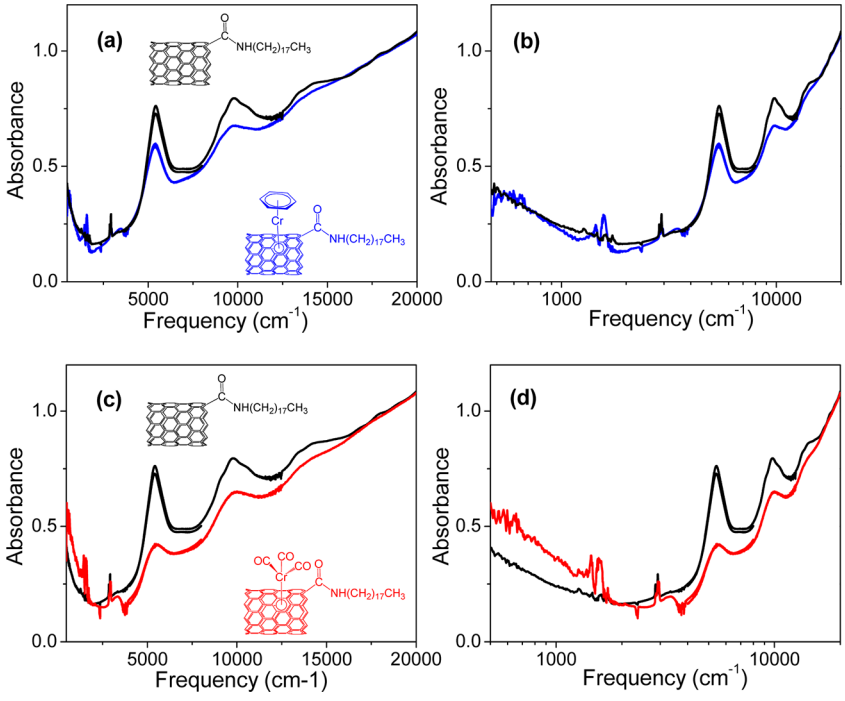

FIGURE 8. IR thin film absorbance spectra of SWNTs functionalized with octadecyl-amine SWNT-$CONH(CH_2)_{17}CH_3$ (black line) and its chromium products: (η^6-SWNT-$CONH(CH_2)_{17}CH_3$)$Cr(C_6H_6)$ (a, b) (blue) and (η^6-SWNT-$CONH(CH_2)_{17}CH_3$)$Cr(CO)_3$ (c, d) (red). Reprinted in part from ref 19. Copyright 2012 Wiley.

A detailed analysis of the thin film spectra in Figure 8 shows that the ratios of the NIR transitions in the functionalized products are reduced to the following percentages of the starting material absorptions: S_{11} = 65%, S_{22} = 54%, M_{11} = 56% for η^6-SWNT-CONH$(CH_2)_{17}CH_3$)Cr(η^6-C_6H_6); S_{11} = 47%, S_{22} = 65%, M_{11} = 56% for η^6-SWNT-CONH$(CH_2)_{17}$-CH_3)Cr$(CO)_3$.[19] Thus, based on our analysis of the spectroscopy of the monohapto-SWNT organometallic derivatives, the hexahapto-metal bond preserves the essential characteristics of the conjugation and the electronic band structure of both the semiconducting and metallic SWNTs, and we further support this contention below, with transport measurements on SWNT thin films which bring into play the bis-hexahapto-metal mode of complexation.

It is convenient to discuss the mode of bonding in these coordination compounds from the standpoint of the bis-hexahapto complexes (Figures 6 and 10d), and the conventional orbital interaction diagram is given in Figure 9 for bis(benzene)chromium [(η^6-$C_6H_6)_2$Cr] (**5**).[46] While the SWNTs provide a number of chiralities, reference to the graphene band structure and FMOs, is instructive (Figures 1 and 2). All of the extended, periodic π-electron graphitic structures are narrow or zero band gap materials and thus the electron-donor and electron-acceptor interactions between the HOMOs and LUMOs of the π-systems, and the d-orbitals of the transition metals will be enhanced by the high lying HOMO and low lying LUMO of the graphitic surfaces, in just the same way that we discussed for the graphene FMOs in the Diels–Alder reactions.[17] Furthermore it may be seen in Figure 9 that the e_{1g} and e_{2u} benzene π-orbitals, which hybridize with the metal d-orbitals and are strongly involved in the construction of the hexahapto-metal-bonds in (η^6-$C_6H_6)_2$Cr, are available at the Dirac point in graphene (Figure 1). Thus the electronic structure of the graphitic π-electron systems is ideally suited for the realization of organometallic chemistry.

5.2. Transport Properties of SWNT Thin Films: Atomic Contacts and Interconnects via the Formation of Bis-Hexahapto-Metal Bonds. In this section of the present Account we review our progress on the high vacuum e-beam evaporation of metals onto SWNT thin films in which the hexahapto-metal bond functions as an electrically conducting interconnect between the side-wall benzene rings of adjacent SWNTs.[19−21] It is important to clearly differentiate the discrete atom, hexahapto-metal-bond from the usual bulk metal contacts and interconnects at graphitic surfaces, which have been shown to dissipate heat, to be limited by the quantum conductance at the junction, and to suffer from charge transfer effects.[13,52]

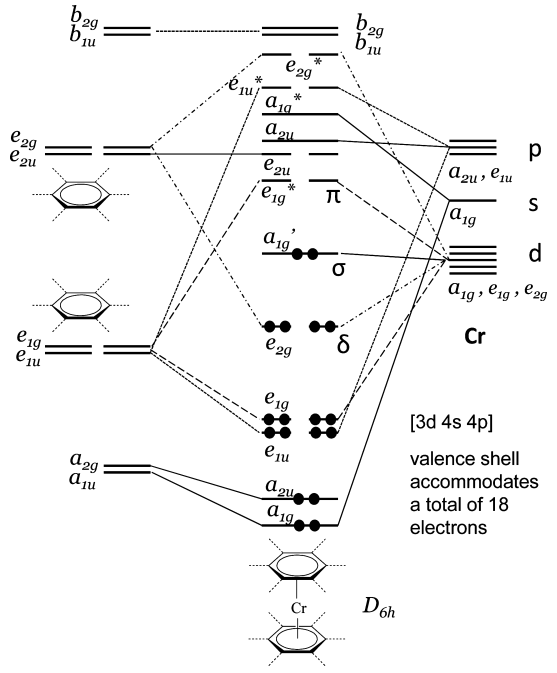

FIGURE 9. Orbital interaction diagram for bis(benzene)chromium, [(η^6-$C_6H_6)_2$Cr].

We have studied electric arc (EA) produced SWNT films, both in the form of the usual statistical 1:2 mixture of metallic and semiconducting SWNTs, and as separated semiconducting SWNTs.[19−21] In order to allow a clear differentiation between the covalent organometallic chemistry discussed above, and the effects of metal to carbon charge transfer, we focus on the results obtained from thin films (thickness $t \approx 8$ nm) of semiconducting (SC) SWNTs which were deposited on interdigitated gold electrodes.[21]

In order to represent the behaviors introduced above, we investigated three reactions with metals (M): (a) weak physisorption (Au), (b) strong physisoption (charge transfer, Li), and (d) chemisorption, with hexahapto complexation (Cr). As may be seen in Figure 10, the deposition of these three metals bring about disparate effects in the conduction behavior of the SC-SWNT films. The response of the SWNT film to gold deposition is very small, despite the fact that the bulk electrical conductivity of gold is about six times that of Cr and Li. The conductance increased by a factor of over 100 on Li deposition and the conductivity of the SC-SWNT film increased monotonically, before reaching a maximum conductivity at about $t \approx 1.2$ nm. The overall response of the SWNT film to the deposition of Cr was not as pronounced as in the case of Li; however, the variation in the conductivity of the SC-SWNT film showed a different dependence on the amount of metal deposited. The amount of Cr needed to achieve its maximum effect on the conductivity of the

SC-SWNT film was extremely small, and for a Cr thickness $t < 0.05$ nm, the conductivity of the SC-SWNT film increased by more than an order of magnitude, whereas for $t =$ 0.05 nm Li, there was a relatively small change in the SC-SWNT film conductivity (Figure 10c).

The conductivity increase observed in the case of Au deposition on the SC-SWNT film can be explained by the parallel conductance of a weakly absorbed, continuous Au film, whereas the Cr and Li depositions involve more complex phenomena. The compositions (MC_x), at the points where the films attained their maximum conductance, were determined to be: $t_M = 1.2$ nm for Li, giving a value of $x \approx 8$ (LiC_8), whereas for Cr the upper limit was reached at $t_M < 0.05$ nm, which gives $x > 180$.

The films consist of a network of individual semiconducting SWNTs and SWNT bundles, and the transport characteristics of the films are dominated by the resistance of the individual semiconducting SWNTs but, more importantly, by the highly resistive nature of the intercarbon nanotube junctions.[53] The increase in the conductivity of SWNTs on exposure to alkali metals has been attributed to charge transfer into the conduction band of the SWNTs to give a composition KC_8, which is reminiscent of the composition of graphite intercalation compounds.[43,44] In the case of Cr deposition, the enhanced film conductivity is ascribed to the reduction of the internanotube resistance due to the formation of a small number of highly conductive bis-hexahapto-metal bonds that serve to bridge individual SC-SWNTs, and thereby reduce the resistance between individual SWNTs and bundles. The chromium atoms are highly mobile,[38,39] and thus, they are able to diffuse along the graphitic surfaces until they encounter a SWNT−SWNT junction or intrabundle contact with a geometry that allows formation of a bis-hexahapto-metal bond (Figure 10d). The formation of a (η^6-SWNT)Cr(η^6-SWNT) bond at a junction is kinetically favorable because the van der Waals gap of 3.15 Å within SWNT bundles is comparable to the separation of 3.23 Å between the benzene rings in dibenzene chromium, $(\eta^6\text{-}C_6H_6)_2Cr$ (**5**).[47] The chromium atom possesses 6 valence shell electrons and by covalent coordination of two η^6-benzenoid ligands shares a total of 18 electrons, which fills the 3d 4s 4p first row transition metal valence shell and it is known to lead to a stable electronic structure.[46] Due to its filled outer d-orbital, gold is unable to participate in hexahapto complexation and cannot provide a conducting pathway at the carbon nanotube junctions; the conductivity increase during gold deposition is ascribed to the parallel conductance of a continuous gold metal film formed over the SWNTs.

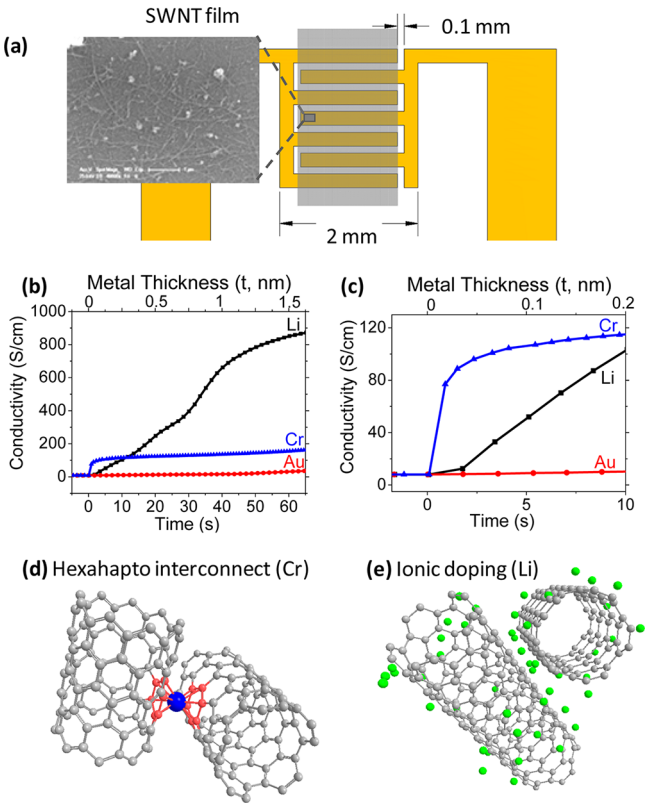

FIGURE 10. (a) Schematic and SEM image of a SC-SWNT thin film on interdigitated electrodes. (b, c) Conductivity of SWNT films as a function of Li, Cr, and Au deposition. (d) Chromium atoms interconnecting adjacent nanotubes by formation of a bis-hexahapto [(η^6-SWNT)Cr-(η^6-SWNT)] linkage, thereby reducing internanotube junction resistance. (e) Electron transfer process (doping), in which lithium atoms donate electrons to the conduction bands of the SWNTs. Reprinted from ref 21. Copyright 2012 American Institute of Physics.

The response of the conductivities of the SC-SWNT films to the deposition of first row transition metals immediately adjacent to Cr in the periodic table is given in Figure 11. These metals (M = Ti, V, Cr, Mn, and Fe) spontaneously form $(\eta^6\text{-}C_6H_6)_2M$ complexes by low temperature metal vapor synthesis (MVS)[46] and are appropriate precursors for intercarbon nanotube junction formation, and it may be seen that they exhibit the same sharp increase in conductivity that was found in the case of chromium. The effect of metal atom deposition on the conductivity of the SWNT thin films decreases in the order: Cr > V, Mn > Fe, Ti (Figure 11).

The electronic structure of the Cr complexes is given in Figure 9; Cr is associated with the stable 18 valence electron count discussed above, and thus, the optimum electronic structure of the bridging complex for intercarbon nanotube hexahapto-metal junctions obeys the familiar 18-electron

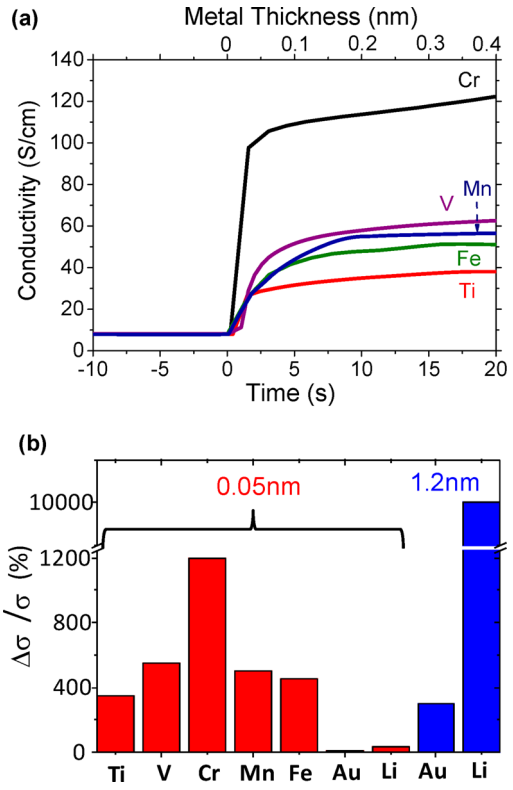

FIGURE 11. (a) Conductivity of SC-SWNT films as a function of metal deposition (M = Ti, V, Cr, Mn, and Fe). (b) Effect of metal atoms deposition on the conductivity of SWNT films. Reprinted from ref 21. Copyright 2012 American Institute of Physics.

rule of organometallic chemistry.[46] We conclude that covalent chemisorption (Ti, V, Cr, Mn, and Fe), in which there is constructive rehybridization, preserves the graphitic band structure and leads to the formation of conductive carbon nanotube interconnects via bis-hexahapto bond formation, and it is apparent that this new mode of bonding to graphitic surfaces may provide a powerful approach for the fabrication of new electronic materials of increased dimensionality.

6. Conclusions and Outlook

In this Account, we illustrate the distinction between covalent chemisorption on graphitic surfaces, which involves σ-bond formation with a fully rehybridized sp^3 carbon atom that is removed from conjugation (destructive rehybridization), and the formation of a bis-hexahapto-metal bond that largely preserves the graphitic band structure (constructive rehybridization). The latter result provides a new approach to the application of covalent bond forming reactions in the modification of the transport properties of graphitic structures, which, unlike previous methodologies, leads to an enhancement in the conductivity by increasing the dimensionality of the electronic structure. It is important to note the distinction between the atomic, chemically formed interconnects discussed in this Account, and those that depend on the physical adsorption of bulk metals and have been labeled as a "performance killer" in the formation of metal/graphene contacts.[52] The development of the organometallic chemistry of graphitic materials offers the potential to generate doped structures by use of transition metals, which deviate from the 18-electron rule, while providing electrical interconnects that are applicable to the bridging of any surface containing the benzenoid ring system, including single-walled carbon nanotubes, graphenes, and other graphitic carbons. In fact, the organometallic approach outlined above may lead to new materials and phenomena and there are potential applications in a number of fields, such as organometallic catalysis[18] and atomic spintronics.[37]

The authors acknowledge financial support from DOD/DMEA under contract H94003-10-2-1003 and NSF-MRSEC through contract DMR-0820382.

BIOGRAPHICAL INFORMATION

Elena Bekyarova obtained her Ph.D. degree in Chemistry from the Bulgarian Academy of Sciences. She is currently an Associate Researcher at the University of California, Riverside. Her research interests include synthesis, properties and applications of carbon nanotubes and graphene with particular focus on the chemistry of these materials and modification of their electronic and magnetic properties.

Santanu Sarkar obtained his M.Sc. degree in Chemistry from the Indian Institute of Technology in Madras. He joined the group of Prof. Robert Haddon at the University of California, Riverside in 2010 for his Ph.D. studies. His current research is focused on the chemistry of graphene, graphite nanomaterials and carbon nanotubes, chemical methods for preparation, exfoliation and processing of graphene and their application.

Feihu Wang received his B.S. and M.S. degrees in applied physics from the University of Science and Technology of China (USTC) in 2004 and 2007, respectively. In 2007 he started his Ph.D. study in experimental physics with Prof. Robert Haddon at the University of California, Riverside. His research is focused on the charge transport and optoelectronic properties of carbon nanotube thin films and graphene. He graduated in 2012 and is presently employed by Intermolecular.

Dr. Mikhail Itkis is Research Professor in the Department of Chemistry and Center for Nanoscale Science and Engineering at the University of California, Riverside. He received a B.A. degree in Physics from Moscow Institute of Physics and Technology in 1970 and a Ph.D. in Physics from Institute of Radio Engineering & Electronics, Russian Academy of Sciences. In 2011, Dr. Itkis was recognized by Thomson Reuters as a world top 100 chemist of the

past decade based on his highly cited publications. His research interests cover physics, material science and applications of low-dimensional materials such as carbon nanotubes, graphene and organic molecular conductors, and especially the optoelectronic properties of such systems.

Dr. Irina Kalinina received M.S. and Ph.D. in Chemistry, at Kazan State University in Russia. She held the position of Senior Researcher at Kazan State University in Russia and Associate Researcher at the University of Rouen in France. She has conducted research in synthetic chemistry for 19 years, including 6 years in the nanotechnology field. Currently she is Assistant Researcher at the University of California, Riverside and her research interests are directed towards novel materials and tools for nanotechnology and cover many aspects of the chemical modification of single-walled carbon nanotubes

Xiaojuan Tian is a Ph.D. student in Chemical Engineering at the University of California, Riverside in the Haddon research group. She received her B.S. from Nankai University in China. Her current research focus is chemical processing and applications of graphite nanoplatelets in thermal management.

Robert C. Haddon is best known for the prediction and discovery of superconductivity in alkali-metal-doped C_{60}; his research group is currently working on the chemistry and applications of carbon nanotubes and graphene (http://haddon.ucr.edu).

FOOTNOTES

*To whom correspondence should be addressed.
The authors declare no competing financial interest.

REFERENCES

1 Berger, C.; Song, Z.; Li, T.; Li, X.; Ogbazghi, A. Y.; Feng, R.; Dai, Z.; Marchenkov, A. N.; Conrad, E. H.; First, P. N.; de Heer, W. A. Ultrathin epitaxial graphite: 2D electron gas properties and a route toward graphene-based nanoelectronics. *J. Phys. Chem. B* **2004**, *108*, 19912–19916.

2 Novoselov, K. S.; Geim, A. K.; Morozov, S. V.; Jiang, D.; Zhang, Y.; Dubonos, S. V.; Grigorieva, I. V.; Firsov, A. A. Electric field effect in atomically thin carbon films. *Science* **2004**, *306*, 666–669.

3 Wu, J. S.; Pisula, W.; Mullen, K. Graphenes as potential material for electronics. *Chem. Rev.* **2007**, *107*, 718–747.

4 Haddon, R. C.; Lamola, A. A. The molecular electronic device and the biochip computer: present status. *Proc. Natl. Acad. Sci. U.S.A.* **1985**, *82*, 1874.

5 Loh, K. P.; Bao, Q. L.; Ang, P. K.; Yang, J. X. The chemistry of graphene. *J. Mater. Chem.* **2010**, *20*, 2277–2289.

6 Bekyarova, E.; Sarkar, S.; Niyogi, S.; Itkis, M. E.; Haddon, R. C. Advances in the chemical modification of epitaxial graphene. *J. Phys. D: Appl. Phys.* **2012**, *45*, 154009(pp 18).

7 Sarkar, S.; Bekyarova, E.; Haddon, R. C. Covalent chemistry in graphene electronics. *Mater. Today* **2012**, *15*, 276–285.

8 Ryu, S.; Han, M. Y.; Maultzsch, J.; Heinz, T. F.; Kim, P.; Steigerwald, M.; Brus, L. E. Reversible basal plane hydrogenation of graphene. *Nano Lett.* **2008**, *8*, 4597–4602.

9 Bon, S. B.; Valentini, L.; Verdejo, R.; Fierro, J. L. G.; Peponi, L.; Lopez-Manchado, M. A.; Kenny, J. M. Plasma fluorination of chemically derived graphene sheets and subsequent modification with butylamine. *Chem. Mater.* **2009**, *21*, 3433–3438.

10 Niyogi, S.; Bekyarova, E.; Hong, J.; Khizroev, S.; Berger, C.; de Heer, W. A.; Haddon, R. C. Covalent chemistry for graphene electronics. *J. Phys. Chem. Lett.* **2011**, *2*, 2487–2498.

11 Sarkar, S.; Bekyarova, E.; Haddon, R. C. Reversible grafting of α-naphthylmethyl radicals to epitaxial graphene. *Angew. Chem., Int. Ed.* **2012**, *51*, 4901–4904; *Angew. Chem.* **2012**, *124*, 4985–4988.

12 Zhang, H.; Bekyarova, E.; Huang, J.-W.; Zhao, Z.; Bao, W.; Wang, F.; Haddon, R. C.; Lau, C. N. Aryl functionalization as a route to band gap engineering in single layer graphene devices. *Nano Lett.* **2011**, *11*, 4047–4051.

13 Frank, S.; Poncharal, P.; Wang, Z. L.; de Heer, W. A. Carbon nanotube quantum resistors. *Science* **1998**, *280*, 1744–1746.

14 Bekyarova, E.; Itkis, M. E.; Ramesh, P.; Berger, C.; Sprinkle, M.; de Heer, W. A.; Haddon, R. C. Chemical modification of epitaxial graphene: spontaneous grafting of aryl groups. *J. Am. Chem. Soc.* **2009**, *131*, 1336–1337.

15 Hong, J.; Niyogi, S.; Bekyarova, E.; Itkis, M. E.; Palanisamy, R.; Amos, N.; Litvinov, D.; Berger, C.; de Heer, W. A.; Khizroev, S.; Haddon, R. C. Effect of nitrophenyl functionalization on the magnetic properties of epitaxial graphene. *Small* **2011**, *7*, 1175–1180.

16 Sarkar, S.; Bekyarova, E.; Niyogi, S.; Haddon, R. C. Diels-Alder chemistry of graphite and graphene: graphene as diene and dienophile. *J. Am. Chem. Soc.* **2011**, *133*, 3324–3327.

17 Sarkar, S.; Bekyarova, E.; Haddon, R. C. Chemistry at the Dirac point: Diels-Alder reactivity of graphene. *Acc. Chem. Res.* **2012**, *45*, 673–682.

18 Sarkar, S.; Niyogi, S.; Bekyarova, E.; Haddon, R. C. Organometallic chemistry of extended periodic π-electron systems: hexahapto−chromium complexes of graphene and single-walled carbon nanotubes. *Chem. Sci.* **2011**, *2*, 1326–1333.

19 Kalinina, I.; Bekyarova, E.; Sarkar, S.; Wang, F.; Itkis, M. E.; Tian, X.; Niyogi, S.; Jha, N.; Haddon, R. C. Hexahapto-metal complexes of single-walled carbon nanotubes. *Macromol. Chem. Phys.* **2012**, *213*, 1001–1019.

20 Wang, F.; Itkis, M. E.; Bekyarova, E.; Sarkar, S.; Tian, X.; Haddon, R. C. Solid-state bis-hexahapto-metal complexation of single-walled carbon nanotubes. *J. Phys. Org. Chem.* **2012**, *25*, 607–610.

21 Wang, F.; Itkis, M. E.; Bekyarova, E.; Tian, X.; Sarkar, S.; Pekker, A.; Kalinina, I.; Moser, M.; Haddon, R. C. Effect of first row transition metals on the conductivity of semiconducting single-walled carbon nanotube networks. *Appl. Phys. Lett.* **2012**, *100*, 223111.

22 Tian, X.; Sarkar, S.; Moser, L. M.; Wang, F.; Pekker, A.; Bekyarova, E.; Itkis, M. E.; Haddon, R. C. Effect of group 6 transition metal coordination on the conductivity of graphite nanoplatelets. *Mater. Lett.* **2012**, *80*, 171–174.

23 Castro Neto, A. H.; Guinea, F.; Peres, N. M. R.; Novoselov, K. S.; Geim, A. K. The electronic properties of graphene. *Rev. Mod. Phys.* **2009**, *81*, 109–162.

24 Whangbo, M.-H.; Hoffmann, R.; Woodward, R. B. Conjugated one and two dimensional polymers. *Proc. R. Soc. London A* **1979**, *366*, 23–46.

25 Ruffieux, P.; Groning, O.; Schwaller, P.; Schlapbach, L.; Groning, P. Hydrogen atoms cause long-range electronic effects on graphite. *Phys. Rev. Lett.* **2000**, *84*, 4910–4913.

26 Bahr, J. L.; Yang, J.; Kosynkin, D. V.; Bronikowski, M. J.; Smalley, R. E.; Tour, J. M. Functionalization of carbon nanotubes by electrochemical reduction of aryl diazonium salts: a bucky paper electrode. *J. Am. Chem. Soc.* **2001**, *123*, 6536–6542.

27 Koehler, F. M.; Jacobsen, A.; Ensslin, K.; Stampfer, C.; Stark, W. J. Selective chemical modification of graphene surfaces: distinction between single- and bilayer graphene. *Small* **2010**, *6*, 1125–1130.

28 Sharma, R.; Baik, J. H.; Perera, C. J.; Strano, M. S. Anomalously large reactivity of single graphene layers and edges toward electron transfer chemistries. *Nano Lett.* **2010**, *10*, 398–405.

29 Boukhvalov, D. W.; Katsnelson, M. I. Tuning the gap in bilayer graphene using chemical functionalization: density functional calculations. *Phys. Rev. B* **2008**, *78*, 085413.

30 Borden, W. T.; Davidson, E. R. Theoretical studies of diradicals containing four pi electrons. *Acc. Chem. Res.* **1981**, *14*, 69–76.

31 Borden, W. T.; Iwamura, H.; Berson, J. A. Violations of Hund's rule in non-Kekule hydrocarbons: theoretical prediction and experimental verification. *Acc. Chem. Res.* **1994**, *27*, 109–116.

32 Yazyev, O. V. Emergence of magnetism in graphene materials and nanostructures. *Rep. Prog. Phys.* **2010**, *73*, 056501.

33 Woodward, R. B.; Hoffmann, R. *The Conservation of Orbital Symmetry*; VCH: Weinheim, 1970; Chapter 3.

34 Fukui, K. Theory of orientation and stereoselection. *Top. Curr. Chem.* **1970**, *15*, 1–85.

35 Houk, K. N. The Frontier Molecular Orbital theory of cycloaddition reactions. *Acc. Chem. Res.* **1975**, *8*, 361–369.

36 Zhu, H.; Huang, P.; Jing, L.; Zuo, T.; Zhao, Y. L.; Gao, X. Microstructure evolution of diazonium functionalized graphene: a potential àpproach to change graphene electronic structure. *J. Mater. Chem* **2012**, *22*, 2063–2068.

37 Avdoshenko, S. M.; Ioffe, I. N.; Cuniberti, G.; Dunsch, L.; Popov, A. A. Organometallic complexes of graphene: toward atomic spintronics using a graphene web. *ACS Nano* **2011**, *5*, 9939–9949.

38 Chan, K. T.; Neaton, J. B.; Cohen, M. L. First-Principles Study of Adatom Adsorption on Graphene. *Phy. Rev. B* **2008**, *77*, 235430.

39 Zan, R.; Bangert, U.; Ramasse, Q.; Novoselov, K. S. Metal-graphene interaction studied via atomic resolution scanning transmission electron microscopy. *Nano Lett.* **2011**, *11*, 1087–1092.

40 Li, E. Y.; Marzari, N. Improving the electrical conductivity of carbon nanotube networks: a first-pronciples study. *ACS Nano* **2011**, *5*, 9726–9736.

41 Banerjee, S.; Hemraj-Benny, T.; Wong, S. S. Covalent surface chemistry of single-walled carbon nanotubes. *Adv. Mater.* **2005**, *17*, 17–29.

42 Balch, A. L.; Olmstead, M. M. Reactions of transition metal complexes with fullerenes (C60, C70, etc.) and related materials. *Chem. Rev.* **1998**, *98*, 2123–2165.

43 Dresselhaus, M. S.; Dresselhaus, G. Intercalation compounds of graphite. *Adv. Phys.* **2002**, *51*, 1–186.

44 Lee, R. S.; Kim, H. J.; Fischer, J. E.; Thess, A.; Smalley, R. E. Conductivity enhancement in single-walled carbon nanotube bundles doped with K and Br. *Nature* **1997**, *388*, 255–257.

45 Haddon, R. C. Electronic Structure, Conductivity and superconductivity in alkali metal doped C60. *Acc. Chem. Res.* **1992**, *25*, 127.

46 Elschenbroich, C. *Organometallics*, third ed.; Wiley-VCH: Weinheim, 2006.

47 Haaland, A. The molecular structure of gaseous dibenzene chromium, $(C_6H_6)_2Cr$. *Acta Chem. Scand.* **1965**, *19*, 4146.

48 Haddon, R. C. Comment on the relationship of the pyramidalization angle at a conjugated carbon atom to the sigma bond angles. *J. Phys. Chem. A* **2001**, *105*, 4164–4165.

49 King, W. A.; Di Bella, S.; Lanza, G.; Khan, K.; Duncalf, D. J.; Cloke, F. G. N.; Fragala, I. L.; Marks, T. J. Metal-ligand bonding and bonding energetics in zerovalent lanthanide, group 3, group 4, and group 6 bis(arene) sandwich complexes. A combined solution thermochemical and ab initio quantum chemical investigation. *J. Am. Chem. Soc.* **1996**, *118*, 627–635.

50 Worsley, K. A.; Kalinina, I.; Bekyarova, E.; Haddon, R. C. Functionalization and dissolution of nitric acid treated single-walled carbon nanotubes. *J. Am. Chem. Soc.* **2009**, *131*, 18153–18158.

51 Hu, H.; Zhao, B.; Hamon, M. A.; Kamaras, K.; Itkis, M. E.; Haddon, R. C. Sidewall functionalization of single-walled carbon nanotubes by addition of dichlorocarbene. *J. Am. Chem. Soc.* **2003**, *125*, 14893–14900.

52 Nagashio, K.; Nishimura, T.; Kita, K.; Toriumi, A. Metal/graphene contact as a performance killer of ultra-high mobility graphene - analysis of intrinsic mobility and contact resistance. *IEEE Int. Electron Dev. Meeting* **2009**, 23.2.1.

53 Hu, L. B.; Hecht, D. S.; Gruner, G. Carbon nanotube thin films: fabrication, properties, and applications. *Chem. Rev.* **2010**, *110*, 5790–5844.